https://doi.org/10.5194/egusphere-2026-984
Preprint. Discussion started: 10 March 2026

Process-based upgrades to the WRF multi-layer green-roof scheme (WRF-MLGR v2.0) and evaluation against field observations

Alireza Saeedi[1], Maria Martinez Mendoza[2], E. Scott Krayenhoff[1], James Voogt[2], Andrea Zonato[3], Sylvie Leroyer[4], Claudia Wagner-Riddle[1]

[1] School of Environmental Sciences, University of Guelph, Canada
[2]Department of Geography and Environment, The University of Western Ontario, Canada
[3]CIMA Research Foundation, Italy
[4]Meteorological Research Division, Environment and Climate Change Canada, Canada

Correspondence to: Alireza Saeedi (saeedia@uoguelph.ca), E. Scott Krayenhoff (skrayenh@uoguelph.ca)

Abstract. Green roofs can moderate urban heat by increasing latent heat flux and reducing sensible heat flux. However, capturing these effects in models depends on accurate representation of key green-roof processes, including substrate heat and moisture transport, soil-vegetation-atmosphere energy and moisture exchanges, interactions with the underlying roof, and drainage. Here we introduce targeted, process-based updates to the green-roof scheme (hereafter, MLGR) within the multi-layer urban canopy model (BEP-BEM) in the WRF mesoscale model to address key limitations in the original formulation. The updates include a non-linear dependence of soil thermal conductivity on moisture, vegetation-modulated surface thermal conductivity, explicit soil-surface evaporation, multi-layer root water uptake for transpiration, and canopy interception with evaporation and dew formation. We evaluate the original and modified MLGR schemes using hourly observations from an extensive sedum roof in London, Canada, for 'summer' (1 July–31 August 2014) and 'fall' (1 September–31 October 2014) periods. We also analyze 11–18 October 2025, when green roof modules were placed directly on the roof deck – which corresponds to the model's lower boundary assumption. Following implementation of the process-based improvements, model–measurement agreement for the conductive heat flux is markedly improved: RMSE is reduced from 105.9 to 24.0 W m^{-2} in summer and from 94.2 to 24.0 W m^{-2} in fall and the model produces more realistic overall green roof energy partitioning. The modified model better captures post-rain increases in latent heat flux (Q_E) and improves the timing and magnitude of daytime turbulent latent and sensible heat flux peaks (Q_E and Q_H). Drainage is reduced relative to the original scheme; however, it remains slightly underestimated during summer and slightly overestimated during fall, and biases persist in surface temperature (warm during the day and cool at night) and in the magnitude and variability of Q_E. Overall, the revised MLGR physics improves surface-flux realism, and future development should focus on developing a more realistic vegetation canopy submodule.

1 Introduction

Rapid urbanization has intensified heat exposure as cities alter the surface energy balance through suppressed evapotranspiration, enhanced heat storage in impervious materials, and complex radiative geometry (Oke, 1982; Grimmond

https://doi.org/10.5194/egusphere-2026-984
Preprint. Discussion started: 10 March 2026

and Oke, 1999; Oke et al., 2017), producing urban heat islands (UHIs) and compounding heat-wave risks (Arnfield, 2003; Li and Bou-Zeid, 2013). Green roofs, engineered vegetated systems atop buildings, have emerged as a practical intervention capable of reducing air temperatures because they repartition turbulent heat exchange, decreasing sensible heat flux (QH) and enhancing (QE) (Oberndorfer et al., 2007; Berardi et al., 2014; Santamouris, 2014; Tabares-Velasco and Srebric, 2012), act as a sink for air pollutants by trapping particulate matter on vegetated surfaces (Rowe, 2011), and provide hydrologic co-benefits when deployed at scale (Berndtsson, 2010; Stovin, 2010; Li and Babcock, 2014). The magnitude and persistence of these benefits depend on climate, roof composition, vegetation traits, and especially substrate moisture (Sailor et al., 2008; Tabares-Velasco and Srebric, 2012; Tabares-Velasco et al., 2012) and irrigation management, which together control the partitioning of net radiation into heat storage, sensible heat and evapotranspiration (Heusinger et al., 2018).

At the building scale, the EnergyPlus "EcoRoof" module introduced a physically based coupling between a plant canopy and an engineered soil substrate, while highlighting the need for more mechanistic hydrology and canopy microclimate formulations (Sailor, 2008; Sailor et al., 2008; Heusinger et al. 2018). Subsequent work showed that sensible-heat reduction depends strongly on water availability, with post-rain evaporation playing a key role in shifting energy partitioning toward latent heat flux and enhanced cooling (Heusinger et al., 2018). At the city scale, urban canopy parameterizations (UCPs) embedded in mesoscale models, single-layer schemes (Kusaka et al., 2001; Yang et al., 2015), and multi-layer approaches such as TEB (Masson, 2000; Hamdi and Masson, 2008) and BEP (Martilli et al., 2002; Salamanca et al., 2011) represent radiative geometry, turbulent exchange, storage, and building–atmosphere feedbacks, enabling scenario testing of rooftop interventions at neighbourhood and city scales (Zonato et al., 2021). These coupled model frameworks have been used to assess how green roofs influence urban temperature and heat mitigation, and how these changes affect building energy demand, in both idealized and real-city applications (Li et al., 2014; Sun et al., 2016; de Munck et al., 2018; Jiang et al., 2025).

Despite this progress, there are two persistent gaps that limit fidelity at urban scales. First, the hydrology and thermophysics of thin, engineered substrates are often simplified in mesoscale implementations relative to detailed building-scale models (Yang et al., 2015; Ribeiro et al., 2021). Second, ensuring strict conservation of energy and water across multi-layer substrate and canopy elements remains challenging in offline tests and coupled WRF runs (Tsiringakis et al., 2019; Lipson et al., 2024). Addressing these issues is essential if we are to translate building-scale realism into robust city-scale modelling of green roof scenarios.

This study advances the state of green-roof representation in the WRF multi-layer urban canopy model (BEP+BEM). A recent process-level evaluation of the WRF-BEP+BEM green roof scheme (Zonato et al., 2021) has identified structural deficiencies in its representation of vegetation and soil processes, including the absence of soil evaporation and lack of canopy radiative buffering, which lead to systematic biases in energy partitioning, pronounced daytime warm biases in surface temperature (T_s), and failure to reproduce the observed diurnal phase and magnitude of Q_E and Q_G (Martinez et al.,

https://doi.org/10.5194/egusphere-2026-984
Preprint. Discussion started: 10 March 2026

2026). These findings motivate the targeted physical upgrades and evaluation presented here. We further develop and evaluate this model (Zonato et al., 2021) by (i) applying a moisture-dependent thermal conductivity that improves soil heat storage and release during high soil water content, (ii) modulating effective surface thermal conductivity as a function of vegetation cover to better capture diurnal heat storage, (iii) adding direct soil evaporation alongside plant transpiration to represent total evapotranspiration, (iv) allowing plant water uptake from all substrate layers rather than the top layer alone, and (v) including interception storage, evaporation, and dew formation on leaves. Together, these changes target the two gaps above: improving flux partitioning and the phase and magnitude of diurnal cycles, including the timing of Q_H, Q_E, and Q_G, while remaining computationally compatible with WRF's BEP+BEM framework and conserving energy and mass.

Our objectives are twofold. First, we document the implementation of new formulations in the green-roof scheme implemented in WRF's multi-layer urban canopy model (BEP+BEM). Second, we evaluate the modified model against observations from a monitored extensive green roof in London, Canada, assessing surface temperature, turbulent latent heat flux, storage heat flux, substrate moisture, and runoff.

2 Methods

2.1 Experimental design

2.1.1 Site and simulation periods

Field observations were collected from a green-roof test array on the rooftop of the Talbot College building at Western University (London, Ontario, Canada). The analysis focuses on the instrumented central portion of the array, which is elevated above the surrounding roof surface to accommodate lysimeters and drainage units. The monitored modules were planted with Sedum spurium and had a total substrate depth of 0.15 m.

This paper evaluates the WRF multi-layer green-roof scheme using observations from 2014 and a focused period in 2025. We analyze two continuous periods in 2014: "summer" (1 July–31 August 2014) and "fall" (1 September–31 October 2014). We also examine 11–18 October 2025, when the heat-flux module was moved from the upper array to a layer of styrofoam insulation above the roof deck, providing a better physical match to the modeled roof–substrate setup for clearer interpretation of measured ground heat flux.

Raw measurements were quality controlled, and time periods affected by instrument malfunction, maintenance, calibration events, or missing data were excluded. For this paper, both the observational time series and the corresponding model output were processed to hourly resolution (hourly means for state variables and fluxes, and hourly totals for precipitation).

https://doi.org/10.5194/egusphere-2026-984
Preprint. Discussion started: 10 March 2026

Further details on the site instrumentation, observational processing, and quality-control procedures are provided in Martinez et al. (2026); readers are referred there for a complete description of the observational dataset.

2.1.2 Simulation development

Atmospheric forcing data were prescribed from observations collected on the roof at, or near, the green-roof array. The forcing time series includes incoming shortwave radiation (W m^{-2}), incoming longwave radiation (W m^{-2}), near-surface air temperature (°C), relative humidity (%), wind speed (m s^{-1}), precipitation (mm; hourly accumulation), and surface air pressure (Pa). Pressure was taken from the nearby London A meteorological station at London International Airport (WMO 71623).

Initial conditions for prognostic substrate temperature and water-content variables were prescribed using the available observations at the initialization time. Geometric and material parameters (e.g., layer depths) were prescribed from site measurements and prior characterization (Martinez et al., 2026; Perelli 2014)

2.1.3 Evaluation metrics

Model performance was assessed against measurements of latent heat flux Q_E (W m^{-2}), surface ground heat flux Q_G (W m^{-2}), surface temperature T_s (°C), and substrate volumetric water content θ (m^3 m^{-3}).

Performance statistics reported in Table 1 include mean absolute error (MAE), root-mean-square error (RMSE), systematic RMSE (RMSEs), unsystematic RMSE (RMSEu), and the refined index of agreement (d) following Willmott et al. (2012).

2.2. Original WRF multi-layer urban canopy model green roof scheme

The WRF multi-layer green-roof scheme represents a vegetated roof as a one-dimensional (vertical) column of soil (growing medium) placed on top of the structural roof. This column simulates the coupled heat and water balances within the green-roof system. Following the formulations of de Munck et al. (2013) and Gutierrez (2015) (as summarized by Zonato et al., 2021), the green roof is discretized into 10 layers spanning a total depth of about 0.3 m.

This model computes the roof's heat and water balances by accounting for net radiation, water added by rainfall and irrigation, evapotranspiration from the vegetation, convective heat exchange with the atmosphere, and the vertical diffusion of heat and moisture within the soil layers. In the original scheme, the model makes an important simplification: it does not distinguish a separate vegetation canopy in terms of radiation exchange, or a distinct canopy air layer for heat and moisture exchange. Instead, the green roof has a single surface and associated temperature which is effectively a soil surface with the ability to transpire (and with substantive thermal admittance, unlike a vegetation canopy). It is this surface that exchanges heat and moisture with the atmosphere and conducts heat downward into the roof/substrate column. Heat transfer within the layers is then calculated based on Fourier diffusion, and for the soil-based roof layers the model uses a moisture-dependent thermal diffusivity (Zonato et al., 2021) :

https://doi.org/10.5194/egusphere-2026-984
Preprint. Discussion started: 10 March 2026

$$\lambda = \begin{cases} \frac{e^{-(\log_{10}|\Psi|+2.7)}}{C_s} \cdot 4.186 \times 10^7, & \text{if } \log_{10}|\Psi| \leq 5.1, \\ \frac{4.1\times10^{-5}}{C_s} \cdot 4.186 \times 10^7, & \text{if } \log_{10}|\Psi| > 5.1. \end{cases} \quad (1)$$

where Ψ is the moisture potential (matric suction; negative under unsaturated conditions), and $C_s = (1 - \theta)\, C_d + \theta\, C_w$ is the volumetric heat capacity of wet soil (J m^{-3} K^{-1}). It is computed as a weighted average of the volumetric heat capacity of dry soil (C_d) and water (C_w), with θ the volumetric water content Zonato et al. (2021).

For hydrology, rainfall (and optional irrigation) is added at the green roof (i.e., soil) surface, and water moves only vertically through the substrate in a one-dimensional column; therefore, lateral subsurface flow is not represented. Any excess water that reaches the drainage layer is removed as drainage. In the baseline scheme, moisture loss to the atmosphere is represented through plant transpiration (controlled by canopy and atmospheric resistances), and the model does not include a separate explicit term for direct soil-surface evaporation. The scheme also does not explicitly track a separate canopy-interception water store.

As discussed by Martínez et al. (2026), the original green roof scheme in the WRF multi-layer urban canopy model exhibits important limitations, particularly in its representation of soil heat flux (Q_g). The model does not correctly reproduce the timing and magnitude of Q_g, and these errors propagate through the surface energy balance, leading to inaccuracies in both the strength and timing of latent (Q_e) and sensible (Q_h) heat fluxes. This issue is traced to the fact that there is no radiative canopy, and the soil layer (which has high thermal admittance relative to vegetation) is the radiatively active surface in the model instead of the vegetation. In the next section we detail several updates to this original model version that correct this problem as well as other model issues, and also add additional functionality and realism.

2.3. Modifications to the WRF multi-layer urban canopy model green roof scheme

To improve the representation of heat and water exchange in the WRF multi-layer green-roof scheme, we implemented five physically based modifications.

2.3.1 Revised soil thermal conductivity (“Ksoil”)

In the original scheme, the substrate soil thermal conductivity, k, was defined as a simple linear function of volumetric water content. This approach tends to overestimate heat conductivity when the soil is very wet, which can make the simulated ground heat flux too large and reduce the diurnal range of surface temperature under wet conditions. To address this, we replaced the linear relationship with a Johansen-type formulation (Johansen, 1975; Peters-Lidard et al., 1998). In this method, the effective soil thermal conductivity, k, is calculated as a weighted combination of the dry and saturated conductivities using the Kersten number, K_e:

https://doi.org/10.5194/egusphere-2026-984
Preprint. Discussion started: 10 March 2026

$$k = k_{dry} + K_e(k_{sat} - k_{dry}) \quad (2)$$

Here kdry is the dry soil thermal conductivity, ksat is the saturated soil thermal conductivity, and K_e is a dimensionless function of the degree of saturation. For dry soils we follow Peters-Lidard et al. (1998), who recommend the following semi-empirical expression for k_{dry} as a function of dry bulk density ρ_b (kg m^{-3}) and mineral density ρ_s (kg m^{-3}):

$$k_{dry} = \frac{(0.135\rho_b + 64.7)}{(\rho_s - 0.947\rho_b)} \quad (3)$$

With ρ_s = 2700 kg m^{-3} for mineral soils. The saturated thermal conductivity ksat is calculated from the volume fractions and thermal conductivities of solids, water, air, and (when present) ice, following the mixture expression of Johansen (1975). The Kersten number K_e is parameterized as a smooth function of liquid water saturation, with different coefficients for coarse and fine substrates, which reduces the sensitivity of k at very low moisture contents. Overall, the updated formulation gives a more realistic shift from dry to wet conditions and reduces the unrealistically high soil heat conduction produced by the original linear method.

2.3.2 Vegetation-dependent surface thermal conductivity ("Heat Storage")

In the original green-roof scheme, the model does not include an explicit vegetation canopy, so it does not represent vegetation cover or the shading effect of plants. This means the soil surface receives the full incoming radiation, which can lead to unrealistically large surface heat storage, particularly in the morning, with associated impacts on morning sensible and latent heat fluxes. To make the simulated surface heat storage more realistic, we added a simple vegetation-dependent formulation to the model that modulates the surface thermal conductivity as a function of vegetation coverage, effectively reducing heat storage/release as vegetation cover increases. Following Peters-Lidard et al. (1997) and Ek et al. (2003), we used a vegetation-dependent effective thermal conductivity at the top soil layer, k_{veg}, which scales the bare-soil conductivity k_{s1} by an exponential function of vegetation cover σ_f:

$$k_{veg} = k_{s1}\exp(-\beta_{veg}\sigma_f) \quad (4)$$

Where σ_f is the fractional vegetative coverage of the roof and β_{veg} is an empirical coefficient. Consistent with offline Noah LSM tests (Ek et al., 2003), β_{veg} was set to 2.0. Corresponding effective thermal conductivities were used within the upper 10 cm of soil for the calculation of heat conduction.

2.3.3 Addition of soil surface evaporation ("Soil Evap")

In the original WRF multi-layer green-roof model, latent heat flux was derived only from plant transpiration, and direct evaporation from the soil surface was not included. This approach is not applicable to scenarios where green roof vegetation

https://doi.org/10.5194/egusphere-2026-984
Preprint. Discussion started: 10 March 2026

fraction drops significantly below 1.0. We used the bulk-transfer approach of Viterbo and Beljaars (1995) to quantify evaporation from the soil/substrate surface. The evaporation rate from the top substrate layer, E_s (kg m^{-2} s^{-1}), is given by:

$$E_s = \frac{\rho}{r_a}[q_L - \alpha(\theta_1) q_{sat}(T_{sk}, p_s)] \quad (5)$$

Where ρ is air density, r_a is the aerodynamic resistance between the surface and the lowest atmospheric model level, q_L is the specific humidity at that level, and qsat(T_{sk}, p_s) is the saturation specific humidity at the surface skin temperature T_{sk} and surface pressure p_s. α(θ_1) is a soil-wetness factor that scales the soil-surface vapor pressure (and thus soil evaporation) from dry to saturated conditions. It is computed from the top-layer water content θ_1, with α ≈ 1 for wet soil and smaller α for drier soil defined as:

$$\alpha(\theta_1) = 0.5[1 - \cos(\frac{\pi\theta_1}{(1.6\theta_{cap})})], \qquad \theta_1 < \theta_{cap}$$
$$\alpha(\theta_1) = 1, \qquad \theta_1 \geq \theta_{cap} \quad (6)$$

where θ_1 is the volumetric water content of the upper soil layer and θ_{cap} the field-capacity value, Viterbo and Beljaars (1995).

2.3.4 Multi-layer transpiration and root water uptake ("Root Uptake")

In the original scheme, plant transpiration draws water only from the thin uppermost soil layer, which can make the surface layer dry too quickly. As a result, when the top layer becomes dry, the model limits transpiration, leading to reduced transpiration and an underestimation of latent heat flux. To address this issue, we introduced a multi-layer root-uptake approach that distributes the transpiration demand across the soil layers based on their available water, assuming that plant roots have good access to all soil layers. Total transpiration E_t (kg m^{-2} s^{-1}) is still computed using the original canopy-resistance formulation, but the fraction taken from layer i is:

$$w_i = \frac{dz_i}{\Sigma_{j=1}^{N} dz_j} \quad (7)$$

where d_{zi} is the thickness of layer i, and the sum is over the N soil layers from which transpiration is allowed to draw water. The transpiration extraction from layer i is then:

$$E_{t,i} = w_i E_t \quad (8)$$

2.3.5 Interception storage, evaporation, and dew formation on leaves ("Intercepted Water")

Finally, we implemented a canopy interception sub-model following Heusinger et al. (2018), whose formulation is based on Cammalleri et al. (2010). This sub-model tracks the canopy water store on the leaves and accounts for both evaporation of intercepted water and dew formation (condensation) on the leaf surfaces, depending on atmospheric conditions. The

https://doi.org/10.5194/egusphere-2026-984
Preprint. Discussion started: 10 March 2026

maximum amount of water that can remain on the leaves (interception storage capacity) is assumed to be proportional to leaf area index (LAI):

$$S_{max} = F_{Smax} \times LAI \tag{9}$$

Here, F_{Smax} (m) is a parameter that depends on leaf inclination and morphological properties. A value of F_{smax} = 0.2 mm was adopted based on measurements conducted for herbaceous species on a mountain meadow in Austria (Wohlfahrt et al. 2006). At each time step, a fraction of the incident precipitation P is intercepted in proportion to vegetation cover σ_f:

$$I = \sigma_f \times P \tag{10}$$

The intercepted water depth on the canopy, S, is updated by adding I. If S exceeds S_{max}, the excess water drips to the top soil layer as D:

$$D = \frac{(S - S_{max})}{\Delta t}, \quad \text{if } S > S_{max}$$
$$D = 0, \quad \text{otherwise} \tag{11}$$

where Δt is the model time step. Water stored on the leaves exchanges moisture with the canopy air through a bulk-transfer formulation of the latent heat flux from intercepted water, L_I (W m^{-2}):

$$L_I = LAI \cdot C_f \cdot L_v \cdot u_{af} \cdot \rho_{af} \cdot (q_{af} - q_{f,sat}) \cdot r \tag{12}$$

In this expression, C_f is a bulk transfer coefficient, L_v is the latent heat of vaporization, u_{af} is wind speed at canopy height, ρ_{af} is air density at canopy height, q_{af} is the specific humidity in the canopy air space, and $q_{f,sat}$ is the saturation specific humidity at foliage temperature. The factor r accounts for the fullness of the interception store:

$$r = \left(\frac{S}{S_{max}}\right)^{\frac{2}{3}} \tag{13}$$

When intercepted water is present on the canopy, a fraction of the leaf area is assumed to be water-covered (r), so transpiration is limited to the remaining dry fraction (1−r); as the interception store evaporates and r decreases, transpiration progressively returns toward its dry-canopy rate. So, transpiration Zonato et al. (2021) is defined as:

$$L_t = LAI \cdot \rho_{af} \cdot L_v \cdot \frac{((q_{af} - q_{f,sat}))}{((r_a + r_s))} \cdot (1 - r) \tag{14}$$

Here r_a is the aerodynamic resistance (Louis, 1979) and r_s is the stomatal resistance.

https://doi.org/10.5194/egusphere-2026-984
Preprint. Discussion started: 10 March 2026

3. Evaluation of the modified WRF multi-layer green roof model

Performance of the original and modified WRF multi-layer green-roof models was assessed against measurements of latent (Q_E) and ground (Q_G) heat fluxes at the surface, surface temperature (T_s), and soil water content (θ), along with a residual estimate of sensible heat flux (Q_H).

Table 1. Performance statistics for the original and modified WRF multi-layer green-roof models during summer and fall. Q_E and Q_G in W m^{-2}; T_s in °C; θ in m^3 m^{-3}.

Model	Season	Metric	Q_E	Q_G	Q_G_daytime	Ts	θ
Modified	Summer	MAE	37.0	17.6	15.1	4.3	0.027
Original	Summer	MAE	45.6	87.4	106.2	3.0	0.021
Modified	Summer	d	0.66	0.35	0.27	0.56	0.640
Original	Summer	d	0.62	-0.69	-0.80	0.69	0.711
Modified	Summer	RMSE	46.2	24.0	22.8	4.8	0.029
Original	Summer	RMSE	83.5	105.9	127.5	3.5	0.024
Modified	Summer	RMSEu	43.8	21.3	18.4	2.0	0.014
Original	Summer	RMSEu	65.1	94.5	70.6	1.8	0.013
Modified	Summer	RMSEs	14.7	11.1	13.5	4.3	0.026
Original	Summer	RMSEs	25.0	47.8	106.2	3.0	0.020
Modified	Fall	MAE	66.2	18.4	16.1	4.4	0.059
Original	Fall	MAE	81.1	76.1	91.7	3.2	0.065
Modified	Fall	d	0.56	0.37	0.34	0.62	-0.324
Original	Fall	d	0.56	-0.61	-0.71	0.72	-0.388
Modified	Fall	RMSE	316.2	24.0	22.4	4.8	0.065
Original	Fall	RMSE	369.7	94.2	113.7	3.7	0.076
Modified	Fall	RMSEu	72.9	21.6	18.3	2.0	0.028
Original	Fall	RMSEu	54.4	87.3	69.7	1.8	0.039
Modified	Fall	RMSEs	307.7	10.3	12.9	4.4	0.059
Original	Fall	RMSEs	365.7	35.4	89.9	3.2	0.066

Note: MAE = mean absolute error; RMSEu = unbiased RMSE; RMSEs = systematic RMSE; d = refined index of agreement per Willmott et al. (2012).

Time series show small warm biases for both modelled surface temperatures (Figs. 1a,b). In both summer and fall, the modified model better captures the amplitude and timing of peak latent heat flux, yielding lower RMSE relative to the original model (Table 1; Fig. 1e–f). For ground heat flux, the observations include a nighttime measurement artifact. All

https://doi.org/10.5194/egusphere-2026-984
Preprint. Discussion started: 10 March 2026

physical green roof modules were placed on styrofoam (except those located on the lysimeter), and the heat-flux modules were located on the 'upper array,' which includes an airspace between the green roof modules and the building roof to accommodate the lysimeters and drainage units. This configuration is atypical for vertical heat-flux measurements in a roof system. The green roof system was also constructed from individual, physically isolated modules, meaning that exposed side boundaries were present and could permit lateral heat losses through the bottom and side boundaries that are not fully captured by the plates. At night, the measured Q_G signal becomes nearly flat and has an unrealistically small magnitude, suggesting that heat loss through the air layer (air gap) beneath the modules and the side boundaries reduces nighttime heat release and largely negates the connection to the underlying roof structure; therefore, the heat flux plates may be largely correct locally, but the modular configuration is not fully representative of a green-roof system, in direct physical contact with the underlying roof structure, as assumed in the green roof model. In contrast, the daytime Q_G behavior is more physically consistent; therefore, we additionally report Q_G_day (daytime-only Q_G) metrics in Table 1. Nevertheless, the air gap may also impact the daytime measurements (further discussed later in this section based on measurements in 2025).

Overall, for Q_G the modified model delivers a clear, season-independent improvement, with significant reductions in total error. The removal of bias evident in the original model simulations (lower RMSE and higher index of agreement; Table 1) is visible in both seasons (Figs. 1c, 1d). This indicates a substantive correction to substrate heat storage, which impacts modelled Q_E and critically, Q_H.

In terms of soil water content (θ), the original model more closely follows the observed temporal variability, especially in summer, yielding lower RMSE and a higher index of agreement (Table 1); however, during fall the modified model tracks the observed values more closely and yields a lower RMSE. The original and modified simulations produce very similar soil water content (θ), and both agree well with the observations, capturing the overall seasonal behavior and the fluctuations observed during summer (Figs. 2d, 3d)

Both models slightly overestimate daytime surface temperature maxima; at night, the modified model shows a stronger cold bias, while the original exhibits a smaller bias (Figs. 2a, 3a). The original model underestimates daytime latent heat flux and largely misses the immediate post-rainfall increase, whereas the modified model better matches both the timing and magnitude of the peaks. In particular, the sharp increase in Q_E after rainfall is clearly seen in the observations but is missed by the original model. By adding evaporation from intercepted water on the foliage, the modified model can now reproduce this post-rainfall boost in latent heat flux. This addition allows the model to respond quickly to wet conditions and better match the observed evapotranspiration peaks (Figs. 2b, 3b). To illustrate the post-rainfall latent-heat-flux response more clearly, Fig. 4 shows an event spanning 15–17 July 2014 (DOY 196–198). Following precipitation on DOY 196, the leaf wetness sensor signal increases sharply, indicating rapid wetting of the sedum canopy surface. At the same time, the modified model produces a strong, short-lived increase in modeled latent heat flux (Q_E), consistent with enhanced evaporation immediately after rainfall (including evaporation of intercepted water on the canopy). As the leaf surfaces dry,

https://doi.org/10.5194/egusphere-2026-984
Preprint. Discussion started: 10 March 2026

both the leaf wetness signal and modeled Q_E decrease. In contrast, the original model shows a much more muted response and largely fails to capture the rapid post-rainfall peak.

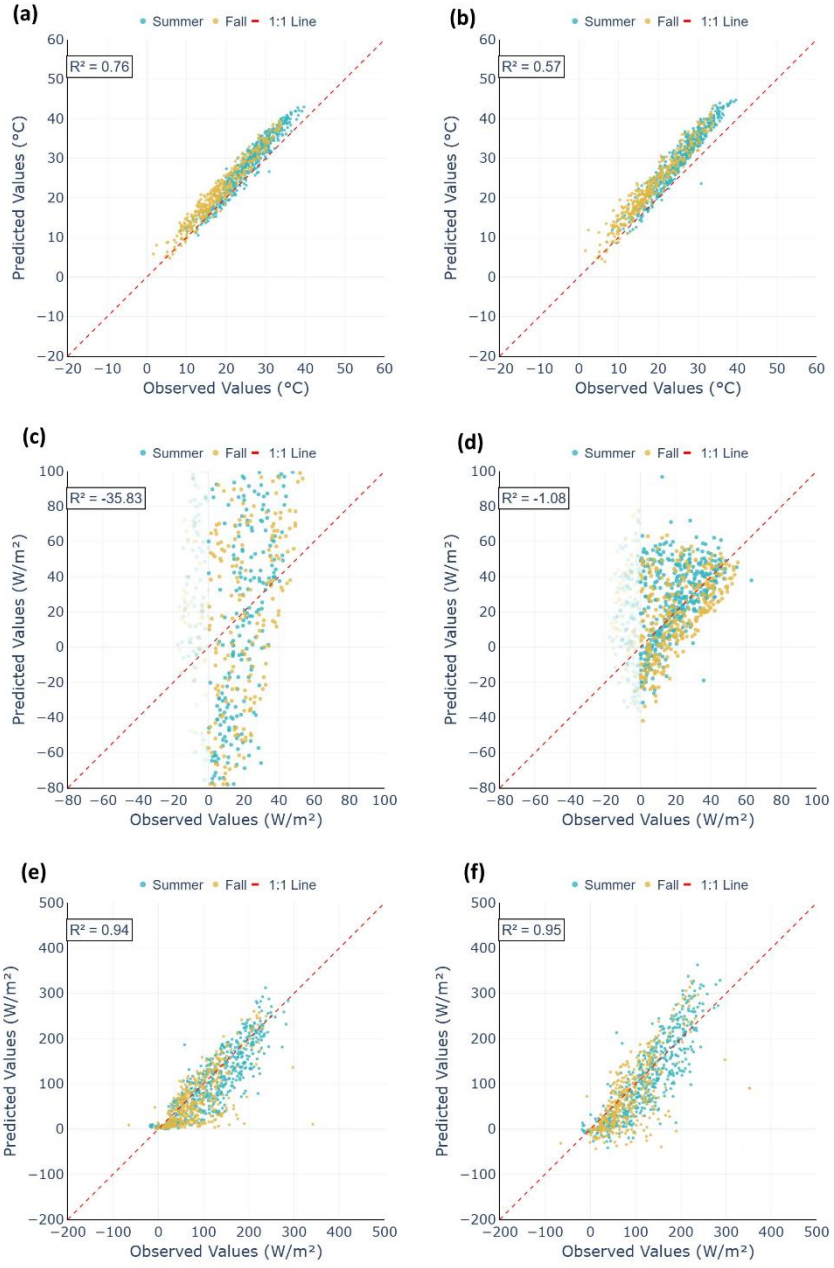

285 **Figure 1.** Comparison of the original model (left column) and modified (right column) multi-layer green-roof model to observations during July 1 to August 31, 2014, and September 1 to October 31, 2014. Panels: (a, b) surface temperature T_s (°C), (c, d) soil heat flux Q_G (W m^{-2}), and (e, f) latent heat flux Q_E (W m^{-2}). Nighttime Q_G points are faded (lighter shading) to indicate reduced confidence in nocturnal Q_G measurement data.

https://doi.org/10.5194/egusphere-2026-984
Preprint. Discussion started: 10 March 2026

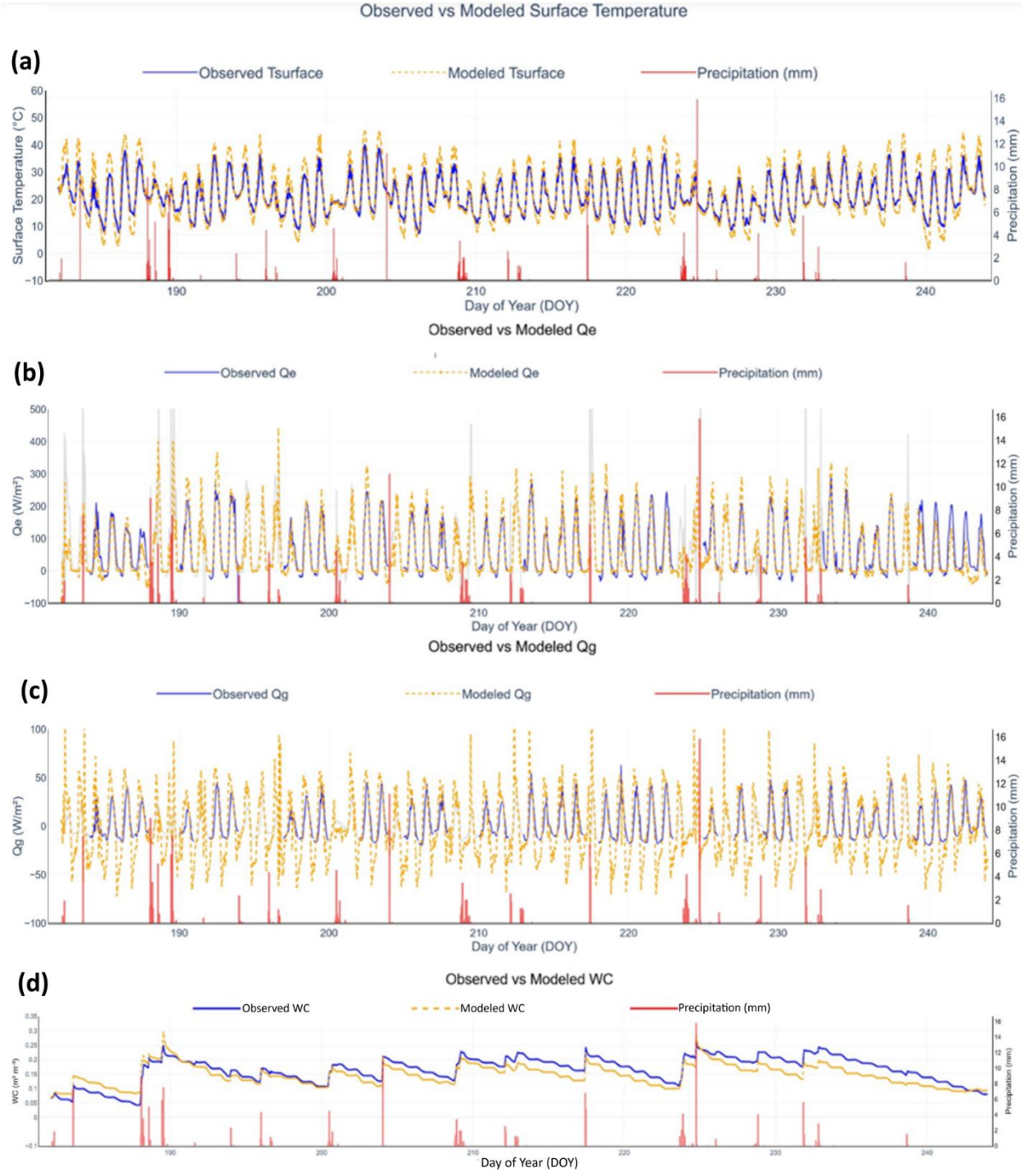

Figure 2. Observed and modified model daily (a) surface temperature T_s, (b) latent heat flux Q_E, (c) ground heat flux Q_G, and (d) volumetric soil water content θ for a period from July 1 to August 31, 2014. In panel (b), gray lines indicate observed latent heat flux during rainy days.

https://doi.org/10.5194/egusphere-2026-984
Preprint. Discussion started: 10 March 2026

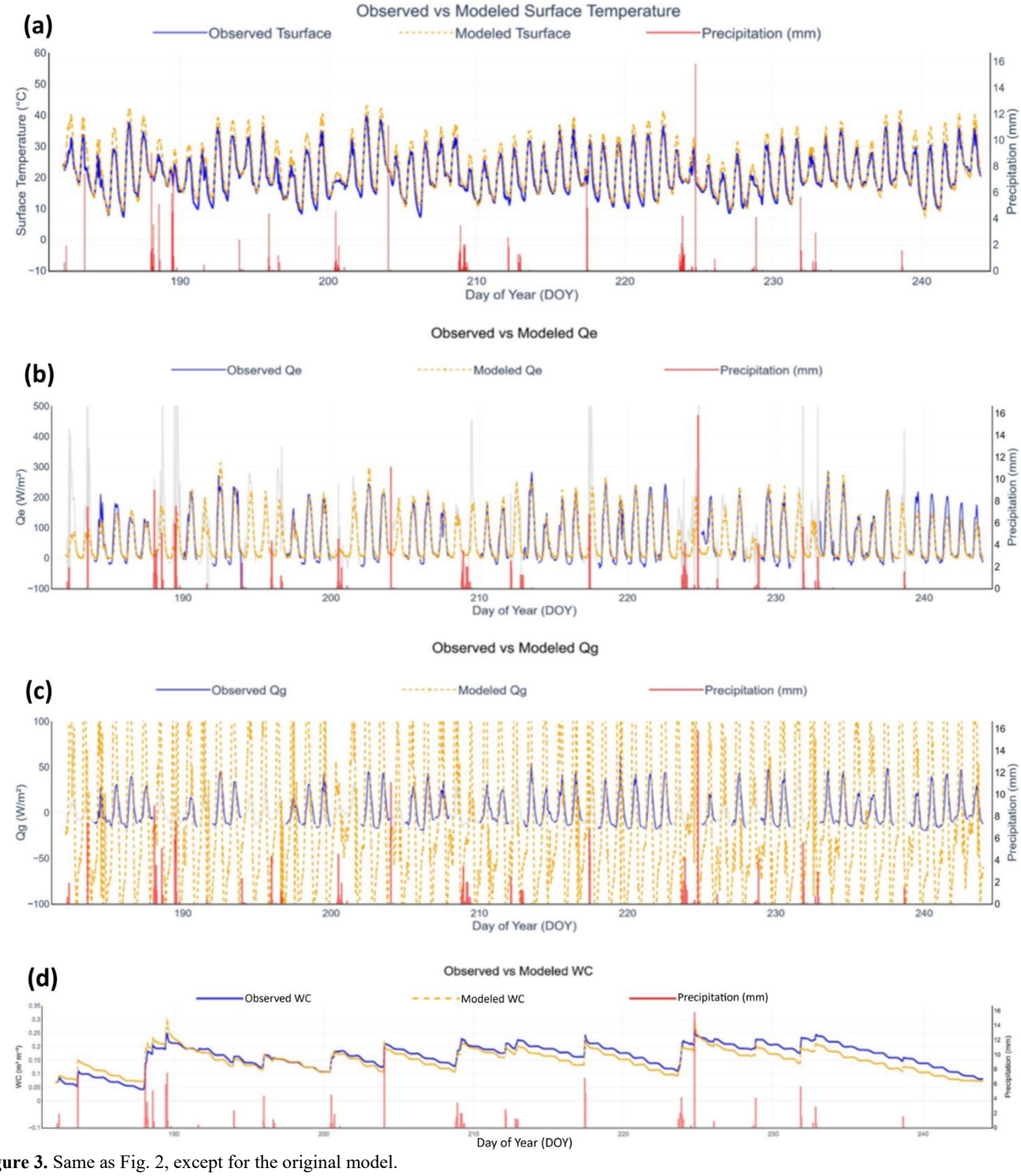

Figure 3. Same as Fig. 2, except for the original model.

https://doi.org/10.5194/egusphere-2026-984
Preprint. Discussion started: 10 March 2026

The most pronounced differences between the model versions appear in the ground heat flux: the modified model damps the exaggerated daytime spikes seen in the original model and exhibits a more realistic nocturnal recovery, consistent with improved substrate thermal conductivity and heat storage—and hence better phase and amplitude (Figs. 2c, 3c). In addition to the long-period evaluation, Fig. 5 shows an event-scale comparison of observed and modeled ground heat flux (Q_G) for 11–18 October 2025 (DOY 284–291), a week with clear observations. During this period, the experimental green-roof module was placed directly on the roof deck (i.e., without an airspace beneath), providing lower-boundary conditions for vertical heat-flux measurements that are both more typical of actual green roofs and which match the model assumptions. Under these conditions, the observed Q_G exhibits a physically consistent diurnal cycle, and the modified model reproduces the main phase and amplitude of Q_G variability, including the daytime peaks and nighttime recovery ($R^2 = 0.642$).

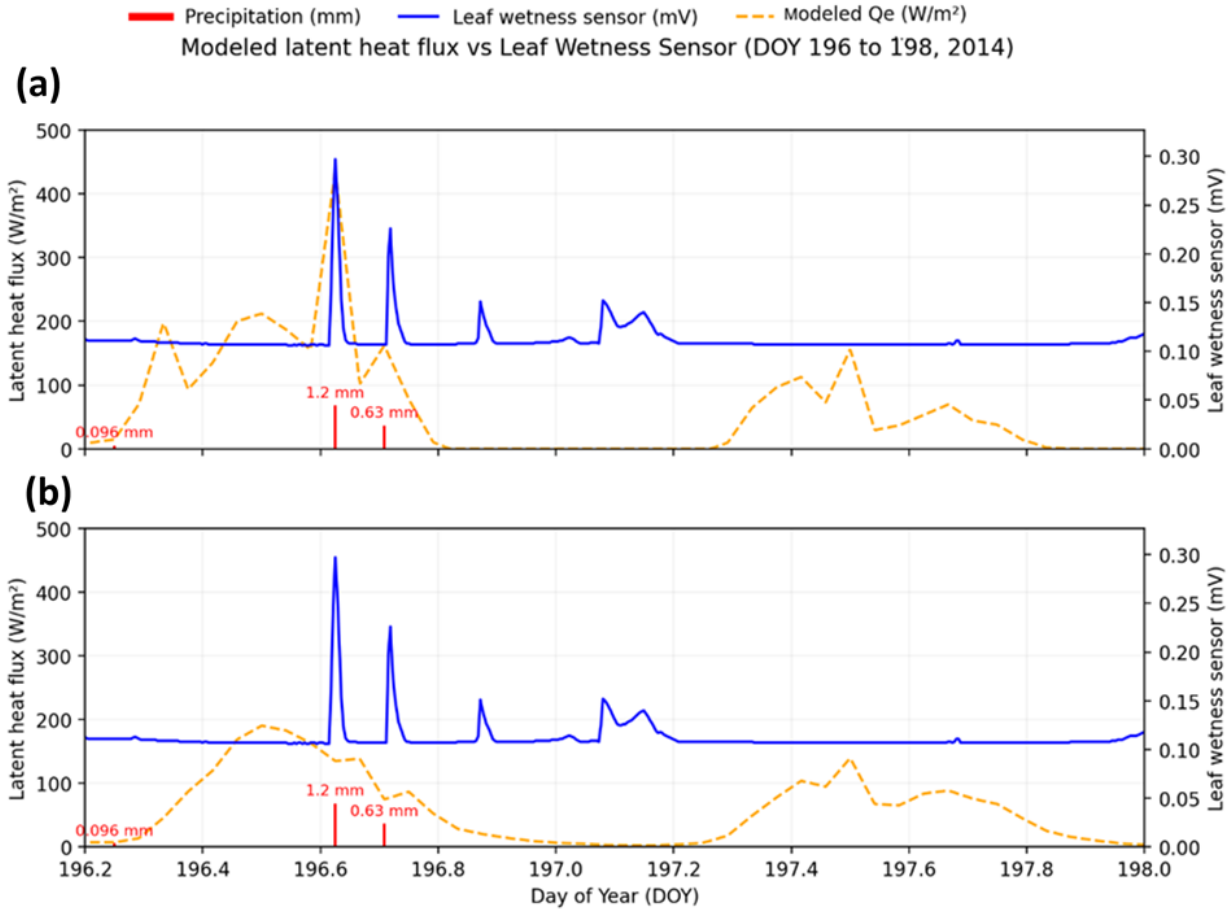

Figure 4. Event-scale comparison of modeled latent heat flux (left axis, W m^{-2}) with leaf wetness sensor signal at the sedum surface (right axis, mV) and precipitation (red bars, mm) for DOY 196–198 (15–17 July 2014). The leaf wetness sensor reports the raw voltage output (mV) from the probe; higher values indicate a wetter surface. Modeled Q_E is shown in dashed orange for (a) modified model and (b) original model.

https://doi.org/10.5194/egusphere-2026-984
Preprint. Discussion started: 10 March 2026

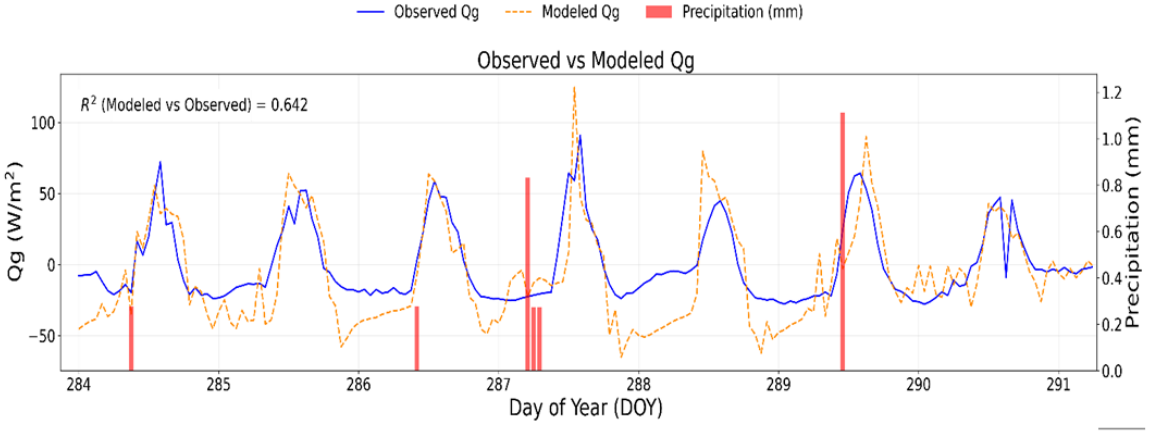

Figure 5. Observed and modeled (modified model) ground heat flux (left axis) and precipitation (right axis) for 11–18 October 2025 (DOY 284–291).

The original model exaggerates the diurnal cycle of Q_G, diverting energy from the turbulent fluxes and depressing morning values as well as midday peaks in Q_E and Q_H (Fig. 6a). Figure 6b demonstrates that the modified model captures both the magnitude and timing of peak latent heat flux Q_E, yielding a realistic daytime partitioning of available energy. The modified model tempers the large positive morning Q_G bias in the original model and as a result better reproduces the timing and amplitude of the daytime peaks of Q_H and Q_E. Differences in Q* are small between the models.

Figures 7 and 8 present a one-at-a-time sensitivity analysis, where each of the five modifications summarized in Table 2 and described in detail in Sect. 2.3 is switched off individually while the other updates remain active. These experiments are used to isolate the role of each added process and to show how the different modifications shape the modelled surface energy partitioning relative to the observations.

In Figure 7, the six panels focus on moisture related processes and how they affect the total latent heat flux (Q_E) in both summer and fall (focus on daytime-only). When multi-layer root uptake is removed (–root uptake; Fig. 7a, b), plants rely primarily on moisture from the uppermost soil layer. As this layer dries during dry-down periods, transpiration becomes increasingly water-limited, leading to a systematic reduction in daytime Q_E, with a clear decrease in the median, particularly in summer, bringing modeled values below both the observations and the fully modified configuration, and a narrowing of the upper distribution. Removing canopy interception storage and its subsequent evaporation (–intercepted water; Fig. 7c, d) suppresses short-lived evaporation pulses following rainfall events, reducing the upper tail of the daytime Q_E distribution and shifting the median to lower values in both summer and fall relative to the observations and the fully modified model. Eliminating explicit soil-surface evaporation (–soil evap; Fig. 7e, f) further decreases daytime Q_E by removing direct evaporation from the exposed soil. In the present simulations, vegetation cover is high (80%), limiting the exposed soil

https://doi.org/10.5194/egusphere-2026-984
Preprint. Discussion started: 10 March 2026

fraction and therefore the magnitude of this effect. Under lower vegetation coverage, however, soil-surface evaporation would contribute more substantially to daytime Q_E, and the sensitivity to this process would be expected to increase.

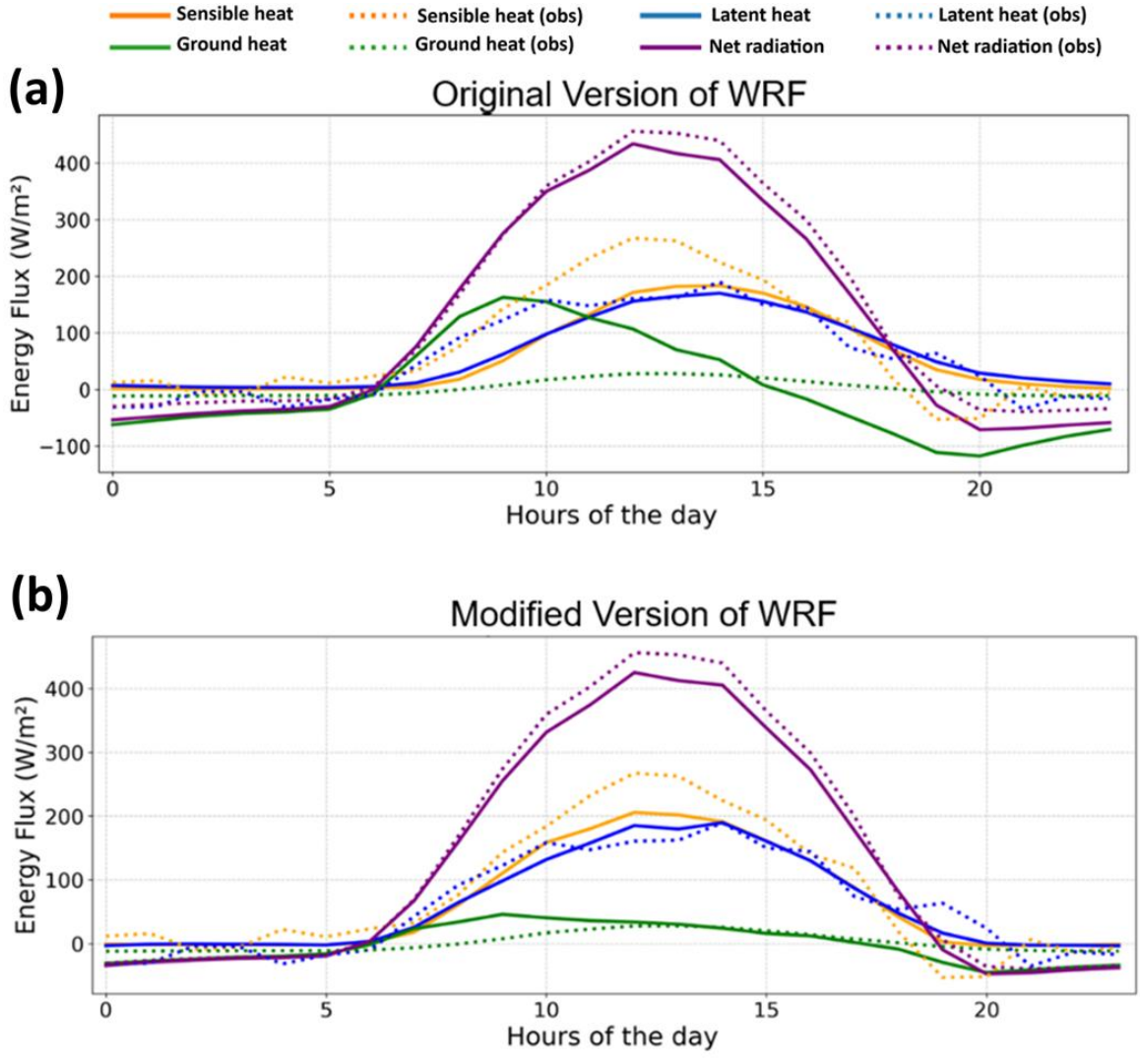

Figure 6. Diurnal mean energy-flux composites for the original model (a) and the modified model (b). Solid lines are model output; dotted lines are observations. Curves are hourly means from July 1 to August 31, 2014.

Figure 8 highlights the thermal-related modifications, which produce the clearest and most systematic sensitivity in the soil heat flux Q_G. Turning off the revised soil thermal-conductivity formulation (–ksoil) causes the Q_G distribution to widen substantially and more extreme values occur, showing that the updated substrate thermal treatment is one of the key controls

https://doi.org/10.5194/egusphere-2026-984
Preprint. Discussion started: 10 March 2026

on soil heat exchange. Removing the vegetation-modulated effective surface thermal conductivity term (–heat storage) also increases the spread and magnitude of Q_G. This modification primarily affects the mean behavior of Q_G by regulating how efficiently incoming radiation is conducted into the substrate. Without vegetation modulation, the roof surface behaves more like bare soil, absorbing and storing a larger fraction of solar energy, which systematically enhances heat storage and leads to stronger daytime Q_G peaks. Together, these results indicate that while the revised substrate thermal conductivity governs the range and extremes of Q_G, the vegetation-dependent surface thermal conductivity plays a dominant role in controlling the mean partitioning of energy into heat storage, thereby reducing persistent biases in Q_G.

Table 2. Summary of one-at-a-time sensitivity experiments in the WRF multi-layer green roof scheme. Short names correspond to titles in Sect. 2 and labels used in Figs. 7–8.

Short name (used in figures)	Description of modification switched off
–root uptake	Multi-layer root water uptake formulation removed; plants extract moisture only from the uppermost soil layer.
–intercepted water	Canopy interception storage and subsequent evaporation disabled.
–soil evap	Explicit soil-surface evaporation term removed.
–ksoil	Revised soil thermal conductivity formulation replaced with the original soil thermal treatment.
–heat storage	Vegetation-modulated effective surface thermal conductivity term removed.

Figure 9 compares the seasonal cumulative drainage over the full observation periods in summer (DOY 182–243) and fall (DOY 244–304) 2014, together with the total observed rainfall during each season. In summer, both model configurations produce slightly lower drainage than observed (45.90 mm), with the original model giving 42.58 mm and the modified model showing a stronger reduction (32.27 mm). In fall, the models generate more drainage than observed (104.90 mm), reaching 128.55 mm in the original model run and 123.72 mm in the modified run. Overall, the seasonal totals highlight a small low bias in summer and an overestimation in fall, while the modified configuration consistently reduces drainage relative to the original model, likely due to its greater ability to evapotranspire due to the “root uptake”, “soil evap” and “intercepted water” modifications.

https://doi.org/10.5194/egusphere-2026-984
Preprint. Discussion started: 10 March 2026

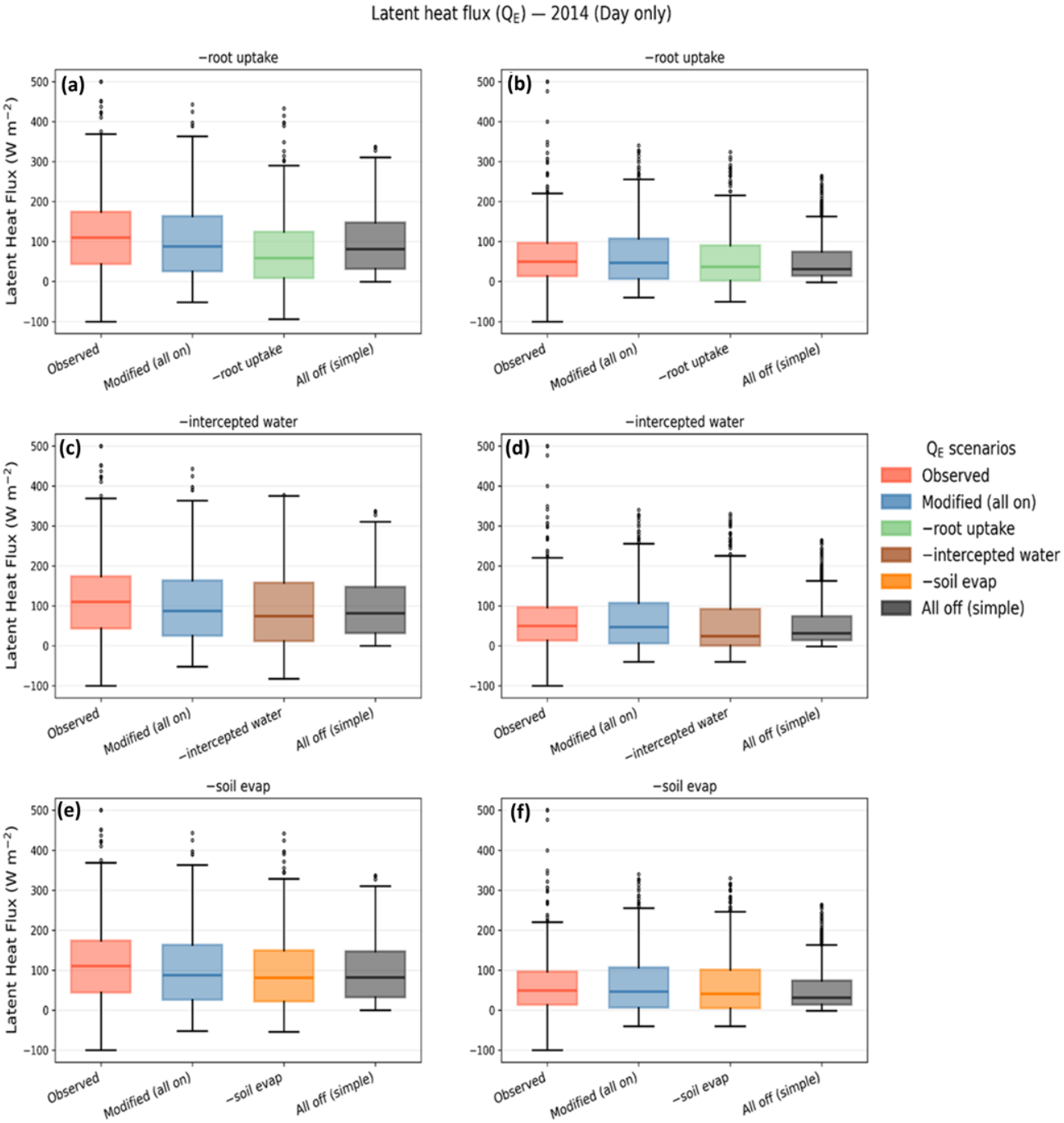

Figure 7. Seasonal distributions of observed and modeled daytime (06:48- 20:02 LST) latent heat flux Q_E for 2014, shown separately for summer (a, c, e; left column) and fall (b, d, f; right column). Panels a and b multi-layer plant water-uptake removed; reverts to the old uptake treatment **(–root uptake)**, panels c and d canopy interception storage and its evaporation removed **(–intercepted water)**, and panels e and f explicit soil-surface evaporation removed **(–soil evap)**. Each panel compares observations with the full modified configuration (all on), the corresponding switch-off experiment, and the original model **(all off)**.

https://doi.org/10.5194/egusphere-2026-984
Preprint. Discussion started: 10 March 2026

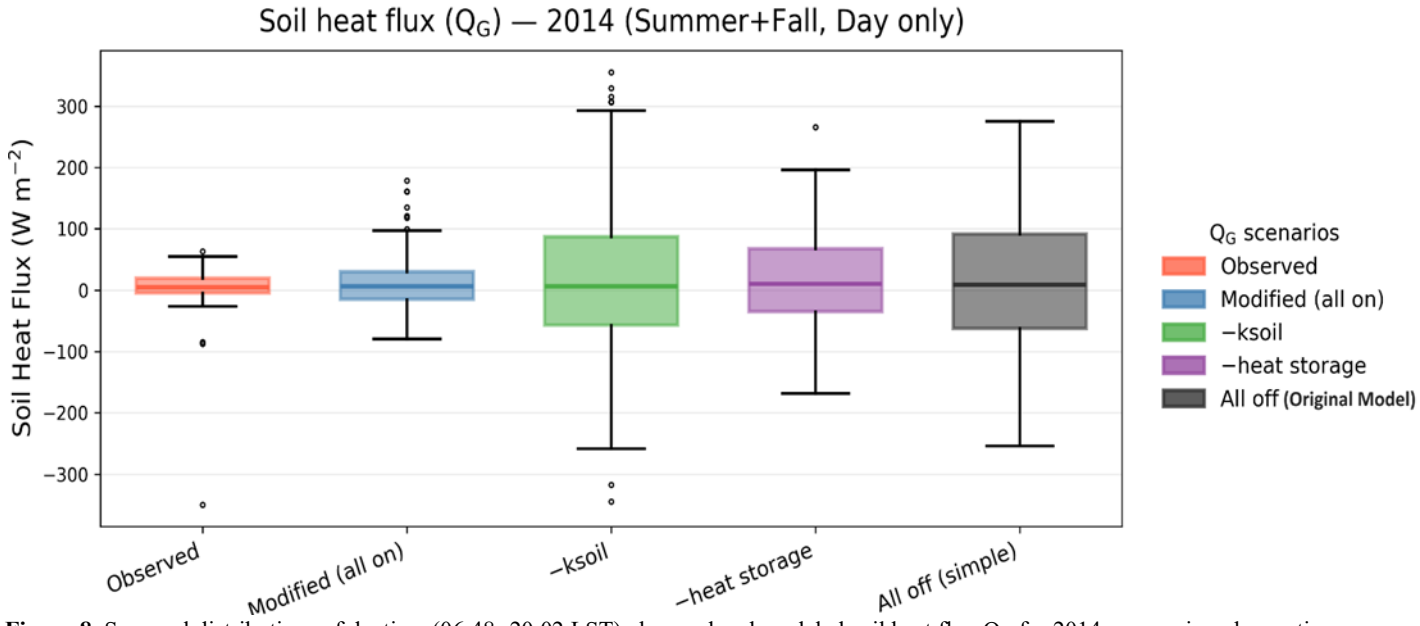

Figure 8. Seasonal distributions of daytime (06:48- 20:02 LST) observed and modeled soil heat flux Q_G for 2014, comparing observations with the modified configuration (all on), –ksoil (new soil thermal-conductivity formulation removed), –heat storage (vegetation-modulated effective surface thermal conductivity term removed), and the original model (all off)

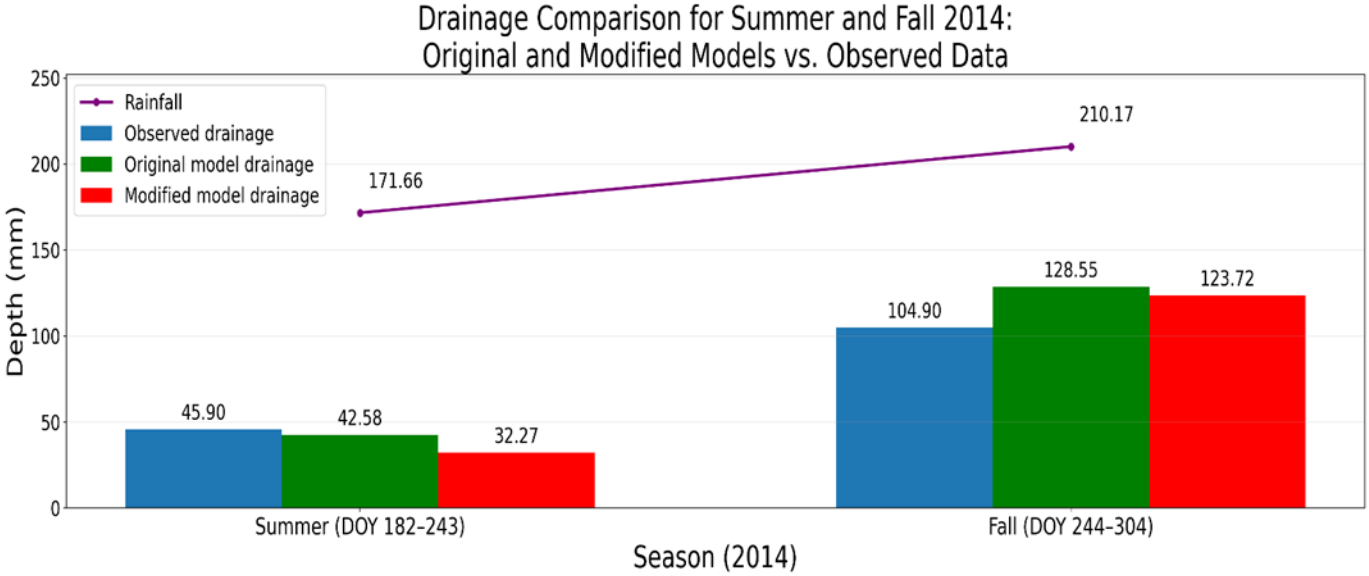

Figure 9. Seasonal totals of observed rainfall (line) and cumulative drainage (bars) for summer (DOY 182–243) and fall (DOY 244–304) 2014. Drainage totals are shown for observations and for the original and modified model configurations.

https://doi.org/10.5194/egusphere-2026-984
Preprint. Discussion started: 10 March 2026

4. Discussion

4.1. Model strengths and residual weaknesses after targeted upgrades

The performance of the modified WRF multi-layer green roof scheme can be evaluated relative to other physically based green roof models. Simulations of extensive green roofs, such as those presented by Heusinger et al. (2018) with a modified version of the EnergyPlus green roof model "EcoRoof", explicitly represent vegetation processes including canopy transpiration, soil evaporation, and evaporation of intercepted water, supported by a detailed canopy microclimate sub-model that resolves radiative and turbulent exchanges between the atmosphere, the canopy, and the surface. Simulations with this modified EcoRoof (ER-modified) model for London indicate that the enhanced canopy microclimate formulation improves surface temperature predictions relative to the original WRF multi-layer green-roof scheme, but with a tendency to overestimate latent and ground heat fluxes (Martinez et al. 2026). Because ER-modified and WRF-MLGR v2.0 are evaluated against the same observational dataset, a direct quantitative comparison can be made. ER-modified demonstrates stronger agreement for surface temperature and ground heat flux, with a index of agreement (d) of 0.77 for Ts and 0.74 for Q_G, when evaluated over the full July–October 2014 period (i.e., combined summer and fall). In comparison, WRF-MLGR v2.0 yields seasonal values of 0.56 (summer) and 0.62 (fall) for Ts and 0.35 (summer) and 0.37 (fall) for Q_G in WRF-MLGR v2.0. In contrast, WRF-MLGR v2.0 exhibits improved skill in simulating latent heat flux, with d values of 0.66 (summer) and 0.56 (fall), exceeding the long-period performance of ER-modified (d = 0.55).

It is relevant to additionally compare other equivalent green roof models. The WRF single-layer green roof representation described in the literature does not document an explicit canopy air space or a dedicated interception storage and evaporation process (Yang and Wang, 2015); however, this model was shown to reproduce surface temperature and turbulent energy fluxes within a reasonable range when evaluated against observations over a 6-day period. Another approach is that the TEB-GREENROOF model directly couples the vegetated substrate to the roof layers without a canopy air space. When evaluated, it showed underestimated substrate moisture, overestimated drainage, and larger than observed temperature amplitudes, reflecting a warm bias and discrepancies in moisture dynamics (de Munck et al., 2013). In the following, we assess the behavior of the modified WRF multi-layer green roof scheme and its strengths, weaknesses, and the impacts of the applied updates.

This study develops a modified version of the WRF multi-layer green-roof scheme and evaluates it against observations in summer and fall of 2014 in London, Canada. The goal of the updates is to address specific process-based limitations identified in the original scheme. In brief, the modified configuration adds (i) a revised non-linear moisture-dependent substrate thermal conductivity formulation (replacing the original linear relationship), (ii) a vegetation-modulated effective surface thermal conductivity term, (iii) explicit soil-surface evaporation, (iv) multi-layer root water uptake, and (v) a canopy interception module that represents interception storage, evaporation of intercepted water, and dew formation on the canopy. Below, we summarize which aspects improve model results most clearly, where key biases remain, and what these results suggest for future development and applications within WRF.

https://doi.org/10.5194/egusphere-2026-984
Preprint. Discussion started: 10 March 2026

Across both seasons, the largest improvement is in ground heat flux (Q_G). In summer, Q_G mean absolute error decreases from 87.4 to 17.6 W m^{-2} and RMSE decreases from 105.9 to 24.0 W m^{-2} (Table 1). In fall, Q_G RMSE decreases from 94.2 to 24.0 W m^{-2} (Table 1). The time series and diurnal plots explain this improvement: the original scheme produces Q_G that swings too strongly, with peaks that are too large during the day and also exaggerated at night, especially an unrealistically sharp morning spike. The modified scheme reduces these exaggerated peaks, so the daily cycle has a more realistic timing and magnitude (Figs. 1–3 and 6).

It is also important to interpret Q_G in the context of the measurement setup. During the 2014 deployment the design of the experimental green roof array provides an elevated platform to allow installation of lysimeters and drainage units below the modules, which also results in an air layer beneath the green roof array. This configuration allows heat to exchange through the bottom (and potentially sides) of the module, which can make the plate-based Q_G measurement harder to interpret—particularly at night, when signals are smaller and boundary effects can be more influential. For this reason, we emphasize a separate one-week period (11–18 October 2025), when the modules were placed directly on the roof deck and the physical setup more closely matched the model's lower-boundary assumption of direct contact between the green roof soil and the roof deck underneath. During this week, the observed Q_G shows a clearer diurnal cycle, and the modified model aligns closely with the measurements in both timing and magnitude (Fig. 5), providing strong evidence that the revised physics substantially improves the simulation of ground heat flux (Q_G) under conditions that best match the model configuration (and the configuration of most actual green roofs).

Reducing the unrealistic daytime Q_G peak also improves how the model partitions energy between the remaining heat-flux terms. With overestimated morning Q_G, the original model reduces the morning and midday latent heat flux (Q_E) and sensible heat flux (Q_H) to compensate. The diurnal plots show this effect clearly: the original model's exaggerated Q_G cycle occurs at the same time as underestimated daytime Q_E and Q_H, while the modified setup captures the timing and size of the Q_E and Q_H peaks more accurately (Fig. 6). Overall, this leads to a more realistic daytime energy partitioning.

A second clear improvement is in the latent flux (Q_E). Figures 2b and 3b show the diurnal cycles with a noticeable increase in Q_E right after rainfall. The original model often represents this response too weakly or misses it, which contributes to an overall underestimation of Q_E during wet periods. In contrast, the modified model captures these short-lived post-rain increases more consistently and provides a better overall prediction of Q_E variability and magnitude. This behavior is especially clear during 15–17 July 2014 (DOY 196–198). Following rainfall, the leaf wetness sensor signal rises sharply, indicating rapid wetting of the sedum canopy surface, and the modified model simultaneously produces a strong, short-lived spike in modeled Q_E. As the leaf surfaces dry, both the sensor signal and modeled Q_E decrease. The original model, however, produces a much weaker response and largely fails to capture this rapid post-rainfall peak (Fig. 4). Overall, this suggests that the modified scheme better represents fast evaporation pathways immediately after wetting, consistent with the inclusion of evaporation from intercepted water on the canopy. The most direct explanation is the added canopy interception module, which allows intercepted water stored on the canopy to evaporate quickly after rainfall (and also represents dew formation), rather than relying only on slower changes in substrate moisture and evaporation. This is consistent with the broader land-

https://doi.org/10.5194/egusphere-2026-984
Preprint. Discussion started: 10 March 2026

surface modeling literature, where interception loss is recognized as an efficient, rapid pathway for returning precipitation to the atmosphere and is often needed to reproduce these short post-rain evaporation responses (e.g., Cammalleri et al., 2010; Heusinger et al., 2018).

Another important improvement comes from the updated root water uptake. In the original scheme, transpiration draws water mainly from the thin top layer, so Q_E drops when that layer dries and more water ends up draining from the bottom of the soil layer. In the modified model, uptake can access moisture from multiple soil layers, which supports more realistic Q_E during dry-down and reduces excess drainage. We also added explicit evaporation from the soil surface. Together, these changes improve the overall energy partitioning. The drainage comparison is consistent with this behavior: the modified model produces less drainage than the original model (Fig. 9). However, drainage remains underestimated in summer and overestimated in fall in both model configurations.

Even with these improvements, some biases remain. First, daytime surface temperature (T_s) is still too warm in both model configurations (Figs. 2a–3a). This suggests that the model may still be restricting heat and moisture exchange, or that some surface and canopy parameters (such as radiative properties, shading, or heat storage) remain overly simplified or incorrectly specified. Second, Q_E is still low and shows less variability than the observations (Fig. 7). The sensitivity tests help explain this: when soil-surface evaporation is removed (–soil evap), and canopy interception storage and its evaporation (–intercepted water) or root uptake is removed (–root uptake), Q_E decreases further and more energy can shift into Q_H and Q_G (Fig. 7). This shows that the added moisture pathways are working as intended. However, the remaining underestimation of Q_E variability suggests that the model still misses some real-world controls, such as microclimatic gradients within the canopy air space and plant physiological responses (for example, a more detailed canopy microclimate). For example, the EnergyPlus green roof (EcoRoof) model represents vegetation as an explicit canopy, including within-canopy radiative exchange (e.g., shading effects) and canopy air exchange processes that regulate evapotranspiration, which may help capture some of the canopy-microclimate controls that are still simplified in the present WRF configuration (Sailor, 2008).

In terms of substrate moisture, the original model better captured the observed temporal variability in volumetric water content (θ) during summer, whereas the modified model showed improved agreement in fall (Table 1). However, both model versions show a small bias in drainage, modestly underestimating summer totals and overestimating fall totals (Fig. 9). During the summer of 2014, conditions were relatively dry, with even the strongest convective rainfall events producing less than 14 mm. In contrast, fall 2014 saw powerful thunderstorms, with notable events exceeding 73 mm of rainfall in just three hours and another event surpassing 45 mm in two hours. This difference in seasonal rainfall intensity helps explain the models biases. During drier summer periods, the models may underestimate drainage since soils rarely reach near-saturation. Conversely, during fall's intense rain events, soil often approach saturation, prompting the models to produce excessive drainage. The modified model produces marginally lower drainage than the original, consistent with the added water-loss pathways through soil evaporation, transpiration via root uptake across all soil layers, and evaporation of intercepted water from the canopy.

https://doi.org/10.5194/egusphere-2026-984
Preprint. Discussion started: 10 March 2026

4.2. Limitations and future work

Several limitations affect how these results should be interpreted and also highlight priorities for future work. The main observational limitation is ground heat flux (Q_G), which needs to be considered in the context of the measurement setup. The design of the experimental green roof array raises the green roof modules above the real roof deck to accommodate lysimeters and drainage units, leaving an air space beneath the modules on the elevated platform. The green roof is also configured as an array of individual modules, rather than a horizontally extensive layer of growing media and plants. This configuration allows additional heat exchange through the bottom and side boundaries that is not fully captured by the heat-flux plates. This effect can influence Q_G during both day and night, but it appears to be more pronounced at night, when the observed Q_G becomes nearly flat and suggests a very small and almost constant heat loss (Section 3.1). Because of these limitations, we report daytime-only Q_G metrics (Q_G_day; Table 1) as an additional evaluation measure, while recognizing that daytime Q_G is also affected to some extent by the same boundary effects. The October 2025 test week, when the heat flux module was placed directly on the roof deck, provides a useful comparison: under more typical boundary conditions, observed Q_G shows a clearer diurnal cycle that is more consistent with expectation, and the modified model reproduces the main timing and magnitude of Q_G variability (Fig. 5).

A related limitation is that the "observed" sensible heat flux (Q_H) is not measured directly. Instead, it is calculated as a residual: net radiation minus the sum of measured Q_E and measured Q_G. This means that any bias in Q_G, during the day and especially at night—will automatically appear as a bias in the residual Q_H, which makes nighttime Q_H comparisons harder to interpret. Importantly, this does not change one of the main conclusion of this study: the modified model dramatically reduces the large Q_G errors seen in the original scheme. Rather, the residual nature of Q_H mainly limits how confidently we can interpret the remaining nighttime Q_H differences as resulting from model physics.

From a model-development perspective, the upgrades in this study are focused on specific processes, but several simplifications remain. Even with the new interception module, the canopy representation is still basic. For example, the scheme does not fully represent a separate canopy microclimate (its own temperature and humidity near the leaves) or detailed radiation exchange within the canopy. It also simplifies how vegetation modifies near-surface aerodynamics, such as wind reduction, roughness, and the resistances that control heat and moisture transfer. Probably most important is separation of the soil surface and canopy radiation and energy balances together with addition of a clearer resistance/aerodynamic formulation. A likely contributor to the surface temperature bias is that the observed canopy surface (as seen by the infrared radiation thermometer) has substantial three-dimensional structure, with a mixture of sunlit and shaded elements during the day, and locally reduced sky-view factors at night that keep sheltered portions of the canopy warmer than exposed upper surfaces. However, the model represents the vegetation canopy as a flat, uniform layer, thus generating an apparent overheat during the day and too much nocturnal cooling relative to the measured values. These additions would likely help reduce the remaining surface-temperature biases (too warm during the day and too cool at night), improve the spread and magnitude of Q_E (Fig. 7), and further improve the daytime heat storage and nighttime release. Incorporating these processes consistent

https://doi.org/10.5194/egusphere-2026-984
Preprint. Discussion started: 10 March 2026

with field studies showing that green-roof energy partitioning depends strongly on soil moisture, vegetation state, and canopy wetness (e.g., Heusinger and Weber, 2017).

Also, this evaluation focuses on warm-season conditions (summer and fall 2014). For Canadian and broader climate applications, cold-season processes may also be important. Future development should include snow accumulation and melt, freezing and thawing of the substrate, and temperature-dependent hydraulic and thermal properties, because these processes can strongly modify wintertime heat exchange and spring moisture availability. In addition, the scheme could be extended to represent green roof uptake of trace gases—such as CO_2 exchange through photosynthesis (e.g., Mirebeau et al. 2025) and a simple deposition/uptake pathway, so the model can also be used to explore potential green-roof impacts on urban air quality.

Finally, since the ground-level vegetation scheme in WRF-BEP+BEM is based on this green roof model, these upgrades can be applied in the future to further improve the accuracy of urban vegetation simulations within that framework.

5. Conclusion

This study introduces targeted process-based modifications to the WRF multi-layer green-roof scheme and evaluates the updated model using field observations from 2014 for continuous summer and fall periods. To better match the model's lower-boundary setup and to interpret ground heat flux (Q_G) more clearly, we also analyze a one-week period (11–18 October 2025) when the green roof modules were placed directly on the roof deck.

The targeted process changes to the green roof model address key limitations in the original scheme. These updates include (i) a revised non-linear, moisture-dependent treatment of substrate thermal conductivity, (ii) a vegetation cover-modulated effective surface thermal conductivity, (iii) explicit soil-surface evaporation, (iv) multi-layer root water uptake, and (v) a canopy interception module that accounts for interception storage, evaporation of intercepted water, and dew formation on the canopy.

Across both seasons, the largest improvement is in ground heat flux (Q_G). In the original scheme, the diurnal Q_G cycle was too strong, with unrealistically large peaks during morning and midday and overly large variations at night. The modified scheme reduces these overestimations and better reproduces both the timing and the magnitude of the daily cycle, leading to much lower Q_G errors (Table 1). This improvement is also supported by the October 2025 test week: when the modules were placed directly on the roof deck, the observed Q_G shows a clearer diurnal pattern, and the modified model matches it closely.

Improving Q_G also ameliorates partitioning of available energy among the remaining surface fluxes. When Q_G is too large, the model directs too much energy into the ground and leaves too little for turbulent exchange, which overly reduces the morning and midday latent heat flux (Q_E) and sensible heat flux (Q_H). By mitigating this unrealistic Q_G draw, the modified scheme reproduces the timing and magnitude of the daytime Q_E and Q_H peaks more accurately. The modified model also represents Q_E more realistically: it captures brief increases in Q_E after rain more consistently, supported by evaporation of intercepted water (including dew-related canopy exchanges), added soil-surface evaporation, and multi-layer root uptake that

https://doi.org/10.5194/egusphere-2026-984
Preprint. Discussion started: 10 March 2026

allows transpiration to draw water from deeper layers. Together, these changes reduce drainage compared with the original model.

Despite this progress, some biases remain. Daytime surface temperature (T_s) is still too warm, nighttime Ts can be too cool, and daytime Q_E is still somewhat low and shows less variability than the observations.

Overall, these results show that the targeted physical updates greatly improve how the WRF MLGR scheme simulates energy and water exchanges, mainly by correcting the substrate thermal treatment as well as adding or modifying select hydrological processes. The modified scheme therefore provides a stronger basis for WRF-based urban climate applications.

Code and Data Availability

The modified and baseline versions of the WRF multi-layer green roof model source code, the input datasets for the 2014 summer and fall evaluation periods, the observational data used for validation, and the post-processing notebooks used to reproduce the figures and evaluation metrics are permanently archived on Zenodo at: https://doi.org/10.5281/zenodo.18704671 (Saeedi et al., 2026).

Author Contributions

AS developed and implemented the updates to the WRF multi-layer green roof model, performed the simulations, and carried out the model evaluation against real-world observations. AS also prepared the manuscript. MM prepared and curated the observational and input datasets used for model evaluation. ESK supervised the project, contributed ideas for model development, and revised the manuscript. JV designed and supervised the observational experiment and revised the manuscript. AZ was the developer of the original WRF multi-layer green roof model described in (Zonato et al., 2021) and provided technical guidance during this study, as well as reviewing and commenting on the manuscript. CWR and SL provided feedback and revised the manuscript. All authors reviewed and approved the final manuscript.

Acknowledgements

This research was funded by the Climate Action and Awareness Fund, administered by Environment and Climate Change Canada. We gratefully acknowledge the contributions of Dimuth Kurukulaarachchi, as well as the 2014 Green Roof research team lead by Dennis O'Caroll, for collecting the observational data used in this study.

Competing interests

The authors declare that they have no conflict of interest.

Financial support

This work was funded by the Government of Canada through Environment and Climate Change Canada (ECCC) under the Climate Action and Awareness Fund (CAAF).

https://doi.org/10.5194/egusphere-2026-984
Preprint. Discussion started: 10 March 2026

References

Arnfield, A. J.: Two decades of urban climate research: a review of turbulence, exchanges of energy and water, and the urban heat island, Int. J. Climatol., 23, 1–26, https://doi.org/10.1002/joc.859, 2003.

Berardi, U., GhaffarianHoseini, A., and GhaffarianHoseini, A.: State-of-the-art analysis of the environmental benefits of green roofs, Appl. Energy, 115, 411–428, https://doi.org/10.1016/j.apenergy.2013.10.047, 2014.

Berndtsson, J. C.: Green roof performance towards management of runoff water quantity and quality: A review, Ecol. Eng., 36, 351–360, https://doi.org/10.1016/j.ecoleng.2009.12.014, 2010.

Cammalleri, C., Agnese, C., Ciraolo, G., Minacapilli, M., Provenzano, G., and Rallo, G.: Actual evapotranspiration assessment by means of a coupled energy/hydrologic balance model: Validation over an olive grove by means of scintillometry and measurements of soil water contents, J. Hydrol., 392, 70–82, https://doi.org/10.1016/j.jhydrol.2010.07.046, 2010.

de Munck, C., Lemonsu, A., Masson, V., Le Bras, J., and Bonhomme, M.: The GREENROOF module (v7.3) for modelling green roof hydrological and energetic performances within TEB, Geosci. Model Dev., 6, 1941–1960, https://doi.org/10.5194/gmd-6-1941-2013, 2013.

de Munck, C., Lemonsu, A., Masson, V., Le Bras, J., Bonhomme, M., and Kounkou-Arnaud, R.: Evaluating the impacts of greening scenarios on thermal comfort and energy and water consumptions for adapting Paris city to climate change, Urban Climate, 23, 260–286, https://doi.org/10.1016/j.uclim.2017.01.003, 2018.

Ek, M. B., Mitchell, K. E., Lin, Y., Rogers, E., Grunmann, P., Koren, V., Gayno, G., and Tarpley, J. D.: Implementation of Noah land surface model advances in the National Centers for Environmental Prediction operational mesoscale Eta model, J. Geophys. Res., 108, 8851, https://doi.org/10.1029/2002JD003296, 2003.

Grimmond, C. S. B. and Oke, T. R.: Heat Storage in Urban Areas: Local-Scale Observations and Evaluation of a Simple Model, J. Appl. Meteorol., 38, 922–940, https://doi.org/10.1175/1520-0450(1999)038<0922:HSIUAL>2.0.CO;2, 1999. American Meteorological Society Journals.

Gutierrez, E.: Quantification of environmental impacts of heat fluxes from built environments, Ph.D. thesis, City University of New York, New York, NY, USA, 2015.

https://doi.org/10.5194/egusphere-2026-984
Preprint. Discussion started: 10 March 2026

Hamdi, R. Hamdi and V. Masson: Inclusion of a drag approach in the Town Energy Balance (TEB) scheme: Offline 1D evaluation in a street canyon, J. Appl. Meteorol. Climatol., 47, 2627–2644, https://doi.org/10.1175/2008JAMC1865.1, 2008.

Heusinger, J. and Weber, S.: Surface energy balance of an extensive green roof as quantified by full year eddy-covariance measurements, Sci. Total Environ., 577, 220–230, https://doi.org/10.1016/j.scitotenv.2016.10.168, 2017.

Heusinger, J., Sailor, D. J., and Weber, S.: Modeling the reduction of urban excess heat by green roofs with respect to different irrigation scenarios, Build. Environ., 131, 174–183, https://doi.org/10.1016/j.buildenv.2018.01.003, 2018.

Jiang, T., Krayenhoff, E. S., Martilli, A., Nazarian, N., Stone Jr., B., and Voogt, J. A.: Prioritizing urban heat adaptation infrastructure based on multiple outcomes: Comfort, health, and energy, Proc. Natl. Acad. Sci. U.S.A., 122, e2411144122, https://doi.org/10.1073/pnas.2411144122, 2025.

Johansen, O.: Thermal conductivity of soils, Ph.D. thesis, University of Trondheim, Trondheim, Norway, 1975.

Kusaka, H., Kondo, H., Kikegawa, Y., and Kimura, F.: A Simple Single-Layer Urban Canopy Model For Atmospheric Models: Comparison With Multi-Layer And Slab Models, Boundary-Layer Meteorol., 101, 329–358, https://doi.org/10.1023/A:1019207923078, 2001.

Li, D. and Bou-Zeid, E.: Synergistic Interactions between Urban Heat Islands and Heat Waves: The Impact in Cities Is Larger than the Sum of Its Parts, J. Appl. Meteorol. Climatol., 52, 2051–2064, https://doi.org/10.1175/JAMC-D-13-02.1, 2013.

Li, D., Bou-Zeid, E., and Oppenheimer, M.: The effectiveness of cool and green roofs as urban heat island mitigation strategies, Environ. Res. Lett., 9, 055002, https://doi.org/10.1088/1748-9326/9/5/055002, 2014.

Li, Y. and Babcock, R. W.: Green roof hydrologic performance and modeling: a review, Water Sci. Technol., 69, 727–738, https://doi.org/10.2166/wst.2013.770, 2014.

Lipson, M. J., et al.: Evaluation of 30 urban land surface models in the Urban-PLUMBER project: Phase 1 results, Q. J. R. Meteorol. Soc., 150, 126–169, https://doi.org/10.1002/qj.4589, 2024.

Louis, J.-F.: A parametric model of vertical eddy fluxes in the atmosphere, Bound.-Layer Meteor., 17, 187–202, https://doi.org/10.1007/BF00117978, 1979.

https://doi.org/10.5194/egusphere-2026-984
Preprint. Discussion started: 10 March 2026

Martilli, A., Clappier, A., and Rotach, M. W.: An urban surface exchange parameterisation for mesoscale models, Boundary-Layer Meteorol., 104, 261–304, https://doi.org/10.1023/A:1016099921195, 2002.

Martinez, M., Saeedi, A., Voogt, J., and Krayenhoff, S.: Process-based evaluation of green roof models for assessment of heat mitigation efficacy in WRF (v4.3.1) and EnergyPlus (v8.6.0), Geosci. Model Dev., under review, 2026.

Masson, V.: A physically-based scheme for the urban energy budget in atmospheric models, Boundary-Layer Meteorol., 94, 357–397, https://doi.org/10.1023/A:1002463829265, 2000.

Mirebeau, A., de Munck, C., Bonan, B., Delire, C., Lemonsu, A., Masson, V., and Weber, S.: Modelling extensive green roof CO2 exchanges in the Town Energy Balance urban canopy model, Geosci. Model Dev., 18, 5329–5349, https://doi.org/10.5194/gmd-18-5329-2025, 2025.

Oberndorfer, E., et al.: Green Roofs as Urban Ecosystems: Ecological Structures, Functions, and Services, BioScience, 57, 823–833, https://doi.org/10.1641/B571005, 2007.

Oke, T. R.: The energetic basis of the urban heat island, Q. J. R. Meteorol. Soc., 108, 1–24, https://doi.org/10.1002/qj.49710845502, 1982.

Oke, T. R., Mills, G., Christen, A., and Voogt, J. A.: Urban Climates, Cambridge University Press, https://doi.org/10.1017/9781139016476, 2017.

Perelli, G. A.: Characterization of the Green Roof Growth Media, M.Eng. Sci. thesis, The University of Western Ontario, London, Ontario, Canada, 2014, Electronic Thesis and Dissertation Repository, 2205, available at: https://ir.lib.uwo.ca/etd/2205.

Peters-Lidard, C. D., Zion, M. S., and Wood, E. F.: A soil-vegetation-atmosphere transfer scheme for modeling spatially variable water and energy balance processes, J. Geophys. Res., 102, 4303–4324,https://doi.org/10.1029/96JD02948, 1997.

Peters-Lidard, C. D., Blackburn, E., Liang, X., and Wood, E. F.: The effect of soil thermal conductivity parameterization on surface energy fluxes and temperatures, J. Atmos. Sci., 55, 1209–1224, https://doi.org/10.1175/1520-0469(1998)055<1209:TEOSTC>2.0.CO;2, 1998.

https://doi.org/10.5194/egusphere-2026-984
Preprint. Discussion started: 10 March 2026

Ribeiro, I., et al.: Highly resolved WRF-BEP/BEM simulations over Barcelona urban area with LCZ, Atmos. Res., 248, 105220, https://doi.org/10.1016/j.atmosres.2020.105220, 2021.

Rowe, D. B.: Green roofs as a means of pollution abatement, Environ. Pollut., 159, 2100–2110, https://doi.org/10.1016/j.envpol.2010.10.029, 2011.

Saeedi, A., Martinez Mendoza, M., Krayenhoff, E. S., Voogt, J., Zonato, A., Leroyer, S., and Wagner-Riddle, C.: WRF-MLGR v2.0: Process-based upgrades to the WRF multi-layer green roof scheme implemented in WRF-BEP+BEM, Zenodo [code], https://doi.org/10.5281/zenodo.18704671, 2026.

Sailor, D. J.: A green roof model for building energy simulation programs, Energy Build., 40, 1466–1478, https://doi.org/10.1016/j.enbuild.2008.02.001, 2008.

Sailor, D. J., Hutchinson, D., and Bokovoy, L.: Thermal property measurements for ecoroof soils common in the western U.S., Energy Build., 40, 1246–1251, https://doi.org/10.1016/j.enbuild.2007.11.004, 2008.

Salamanca, F., Martilli, A., Tewari, M., and Chen, F.: A Study of the Urban Boundary Layer Using Different Urban Parameterizations and High-Resolution Urban Canopy Parameters with WRF, J. Appl. Meteorol. Climatol., 50, 1107–1128, https://doi.org/10.1175/2010JAMC2538.1, 2011.

Santamouris, M.: Cooling the cities – A review of reflective and green roof mitigation technologies to fight heat island and improve comfort in urban environments, Sol. Energy, 103, 682–703, https://doi.org/10.1016/j.solener.2012.07.003, 2014.

Stovin, V.: The potential of green roofs to manage urban stormwater, Water Environ. J., 24, 192–199, https://doi.org/10.1111/j.1747-6593.2009.00174.x, 2010.

Sun, T., Grimmond, C. S. B., and Ni, G.-H.: How do green roofs mitigate urban thermal stress under heat waves?, J. Geophys. Res.: Atmospheres, 121, 5320–5335, https://doi.org/10.1002/2016JD024873, 2016.

Tabares-Velasco, P. C. and Srebric, J.: A heat and mass transfer model for assessment of plant-based roofing systems in summer conditions, Build. Environ., 49, 310–323, https://doi.org/10.1016/j.buildenv.2011.07.019, 2012.

https://doi.org/10.5194/egusphere-2026-984
Preprint. Discussion started: 10 March 2026

Tabares-Velasco, P. C., Zhao, M., Peterson, N., Srebric, J., and Berghage, R.: Validation of predictive heat and mass transfer green roof model with extensive green roof field data, Ecol. Eng., 47, 165–173, https://doi.org/10.1016/j.ecoleng.2012.06.012, 2012.

Tsiringakis, A., Steeneveld, G.-J., Holtslag, A. A. M., Kotthaus, S., and Grimmond, S.: On- and off-line evaluation of the single-layer urban canopy model in London summertime conditions, Q. J. R. Meteorol. Soc., 145, 1474–1489, https://doi.org/10.1002/qj.3505, 2019.

Viterbo, P. and Beljaars, A. C. M.: An improved land surface parameterization scheme in the ECMWF model and its validation, J. Climate, 8, 2716–2748, https://doi.org/10.1175/1520-0442(1995)008<2716:AILSPS>2.0.CO;2, 1995.

Willmott, C. J., Robeson, S. M., and Matsuura, K.: A refined index of model performance, Int. J. Climatol., 32, 2088–2094, https://doi.org/10.1002/joc.2419, 2012.

Wohlfahrt, G., Bianchi, K., and Cernusca, A.: Leaf and stem maximum water storage capacity of herbaceous plants in a mountain meadow, J. Hydrol., 319, 383–390, https://doi.org/10.1016/j.jhydrol.2005.06.036, 2006.

Yang, J., Wang, Z.-H., Chen, F., Miao, S., Tewari, M., Voogt, J. A., and Myint, S.: Enhancing hydrologic modelling in the coupled WRF–urban modelling system, Boundary-Layer Meteorol., 155, 87–109, https://doi.org/10.1007/s10546-014-9991-6, 2015.

Zonato, A., Martilli, A., Gutierrez, E., Chen, F., He, C., Barlage, M., … and Giovannini, L.: Exploring the effects of rooftop mitigation strategies on urban temperatures and energy consumption, JGR Atmospheres, 126, e2021JD035002, https://doi.org/10.1029/2021JD035002, 2021.